Chemical Engineering Science 93 (2013) 257–265

Contents lists available at SciVerse ScienceDirect

Chemical Engineering Science

journal homepage: www.elsevier.com/locate/ces

Remotely excited magnetic nanoparticles and gas–liquid mass transfer in Taylor flow regime

Pouya Hajiani, Faïçal Larachi *

Chemical Engineering Department, Laval University, Québec, QC, Canada G1V 0A6

HIGHLIGHTS

- MNPs are maneuvered at inaccessible liquid film in Taylor flow using magnetic field.
- Spinning MNPs under RMF transfer momentum to surrounding liquid molecules.
- Magnetically-induced nanoconvection enhances k_La in capillary Taylor flow regime.
- Magnetically pinned MNPs weaken gas–liquid mass transfer in Taylor flow regime.

GRAPHICAL ABSTRACT

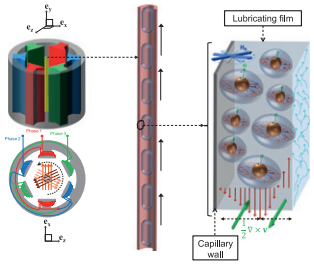

ARTICLE INFO

Article history:
Received 3 August 2012
Received in revised form
23 January 2013
Accepted 26 January 2013
Available online 1 February 2013

Keywords:
Nanomixing
Magnetic nanoparticle
(Uniform DC, AC, rotating) magnetic field
Multiphase flow
Absorption, mass transfer enhancement
Taylor flow regime

ABSTRACT

Gas–liquid mass transfer from oxygen Taylor bubbles to liquid in tube was studied using dilute colloidal suspensions of magnetic nanoparticles (MNPs) as the liquid phase. The tube was hosted inside the bore of a tubular two-pole three-phase magnet and the MNPs were remotely excited by subjecting them to different types of magnetic fields. The influence of magnetic field on the liquid side volumetric mass transfer coefficient (k_La) was cast as an enhancement factor with respect to the magnetic field free base case. The repercussions of magnetic field frequency, MNP concentration, tube alignment and gas velocity on this enhancement factor were measured experimentally. Experimental results suggested that spinning nanoparticles under transverse rotating magnetic fields (TRMF) improved mixing in the lubricating film that surrounds Taylor bubbles which reflected in a measurable enhancement of k_La. On the contrary, axial stationary magnetic fields (ASMF) pinned MNPs translating in systematically degraded gas–liquid mass transfer rates whereas axial oscillating magnetic field had no detectable effects on the mass transfer coefficient.

1. Introduction

Taylor flow in a single tube or in microchannels is identified as the alternating movement of equally long Taylor bubbles separated by liquid slugs (Hessel et al., 2005). Taylor flow could be regarded as a top priority to study *in lieu* of other gas–liquid flow patterns prevailing in microchannels (Yue et al., 2007) owing to its interesting features. For instance, the axial dispersion in the liquid phase is significantly decreased as the only means for material exchange between two adjacent liquid slugs is through the thin liquid film between bubbles and the tube wall "lubricating film" (Trachsel et al., 2005). Moreover, the recirculation motion induced in the liquid slug, which is trapped between two consecutive bubbles, improves radial mass transfer (Gunther et al., 2004; Zaloha et al., 2012). The remarkably high gas–liquid mass transfer rates observed in Taylor flow regime is one additional feature which attracts attentions towards multiphase microchannel systems. Consequently, gas–liquid microreactors have been utilized in a variety of chemical and physical applications including, direct formation of hydrogen peroxide (Ng et al.,

* Corresponding author. Tel.: +1 418 656 3566; fax: +1 418 656 5993.
E-mail address: faical.larachi@gch.ulaval.ca (F. Larachi).

0009-2509/$ - see front matter © 2013 Elsevier Ltd. All rights reserved.
http://dx.doi.org/10.1016/j.ces.2013.01.052

2010; Wang et al., 2007), Pd-catalyzed carbonylation (Gong et al., 2012), direct fluorination (De Mas et al., 2009; Lang et al., 2012), and gas absorption (Sato and Goto, 2004; TeGrotenhuis et al., 2000).

On the other hand, magnetic nanoparticles (MNPs) have found extensive applications in a broad range of scientific disciplines. In the realm of chemistry and chemical engineering, for example, they have been used vastly in homogeneous–heterogeneous (bio)catalysis and (bio)separations (Du et al., 2012; Fu et al., 2012; Hudson et al., 2012; Kong et al., 2012; Liu et al., 2012; Ngo et al., 2012; Xu et al., 2012; Zhang et al., 2012a, 2012b; Zhu and Wei, 2012). Recently, suspended MNPs in aqueous media have been shown to constitute a novel mixing agent in capillary flows upon excitation by magnetic fields. This effect was demonstrated by promoting or retarding lateral mixing in laminar Poiseuille flows (Hajiani and Larachi, 2012). By delivering their magnetic energy cargo via MNP stimulation anywhere into the liquid, a new portfolio of process intensification applications in chemical reaction engineering is foreseen to open up.

For this new class of nanomixing stimulation, an external magnetic field exerts a magnetic torque on the magnetic moment of MNPs suspended in a liquid in order to orient the nanoparticles to align with the magnetic field direction (Rosensweig, 1997). For MNPs, whose magnetic moment is locked in the particle solid crystal lattice (rdMNPs), the magnetic torque is felt bodily leading to a momentum transfer from nanoparticle to the adjacent liquid phase (Rosensweig, 1997). This magnetic body torque is opposed by Brownian collisions from solvent molecules and flow-field hydrodynamic torque particularly when the liquid suspension and the magnetic field are in relative motion (Rosensweig, 1997). Interestingly, the nature of mechanical interactions between magnetically excited MNPs and the liquid depends on the characteristics of applied magnetic field. For instance, when a stationary magnetic field (SMF) is imposed over MNP suspensions in convective motion while fluid vorticity vector ($1/2\nabla \times \mathbf{V}$) is not parallel with MNP spin vector, rdMNPs, pinned by the magnetic field, resist against gyration under hydrodynamic torque that originates from fluid vorticity. This phenomenon, first observed by Rosensweig et al. (1969) and McTague (1969) gives rise to an inflated apparent viscosity called magnetoviscosity (Rosensweig, 1997).

Alternatively, when the magnetic angular torque is exerted on MNPs by a time varying magnetic field, such as a rotating magnetic field (RMF), it causes the suspended rdMNPs to gyrate individually inside the contiguous liquid. A uniform RMF, which emerges from superposition of three, 120° out of phase OMFs, has a constant intensity over time while it changes its direction continuously at any point of the domain. In a quest to catch-up with RMF direction, suspended rdMNPs spin in a direction primarily imposed by RMF (Rosensweig, 1997).

Another type of time varying magnetic field is the oscillating magnetic field (OMF) characterized by an external magnetic field vector ($\mathbf{H}_0$) which changes as a sine-wave with time at each point of the space. Variable magnetic field strength and reversal of $\mathbf{H}$ direction at each wave cycle are two main features that distinguish OMF from RMF. Consequently, OMF and RMF MNP spin mechanisms are expected to be quite different. For instance, in restless MNP suspension ($1/2\nabla \times \mathbf{V} \neq \mathbf{0}$) subject to OMF, the nanoparticle spin direction under magnetic field is imposed in part by the direction of local fluid vorticity surrounding the particle (Shliomis and Morozov, 1994). This process may per se affect both characteristics and quality of mixing induced in OMF conditions.

In this contribution, we attempt to broaden the scope of MNP-mediated mixing toward the Taylor flow regime as the most commonly observed gas–liquid regime in microchannels (Kashid et al., 2011). Although in such contactors radial mixing is improved in the vortex region due to the recirculation patterns within liquid slug, molecular diffusion seems to play a prominent role in the micron-size thin lubricating film which encloses the bubbles (Vandu et al., 2005). The goal of this work is to unveil how magnetic nanoparticles (seeded in liquids at quite dilute levels), stimulated by different moderate-strength magnetic field types, while interacting with shear flow may affect the gas–liquid mass transfer phenomenon in the thin liquid film in Taylor flow regime. In this study, we carried out oxygen absorption from rising Taylor bubbles of pure oxygen into MNP suspensions as a model for gas–liquid mass transfer experiments in a tube. Varying concentrations of nanoparticles in presence/absence of external magnetic field effects were studied. By positioning the tube inside the magnet bore so as to provide the desired MNP spin plane, the magnetic nanoparticles were excited with three different types of magnetic fields, i.e., rotating magnetic field (RMF), oscillating magnetic field (OMF) and static magnetic field (SMF). The tube diameter, gas and liquid flow rates were chosen such that saturation of lubricating film (evaluated from literature correlation of Vandu et al. (2005)) was avoided.

2. Experimental

2.1. Magnet

A tubular two-pole three-phase magnet with bore dimensions of 55 mm height and 45 mm inner diameter was designed and fabricated in collaboration with MotionTech LLC and Windings Inc (Fig. 1a and b). It was used to generate different magnetic field types including RMF, OMF and SMF with moderate magnetic field intensity at the center axis (up to 50 mT). Three identical coil pairs that constitute the magnet assembly can be energized separately or jointly in various configurations as depicted in Fig. 3a, Figs. 4c and 5a. Since RMF emerges from superposition of three OMFs that are 120° out of phase, the coils were fed by three balanced AC currents from a variable frequency drive (ABB, ACS150, 2.2 kW) to generate RMF (Fig. 3a). To impose an OMF, two adjacent coils were energized with an AC current from an AC variable frequency drive (Invertek Drives, Optidrive E2) as shown in Fig. 4c. The coils having the same configuration were connected to a DC current from a DC source (Agilent Tech, N8739A) to provide a SMF as illustrated in Fig. 5a. The magnetic field strength and frequency was adjustable directly by power supplies. The temperature of the magnet solid part was controlled by a water cooling jacket encompassing the outer shell of the stator and filled with a coolant circulated in and out from a constant-temperature thermostated bath (Lauda, Model RKT20). Hajiani and Larachi (2012) can be referred to for further information on the magnet design and specifications.

2.2. Colloidal suspension

Dilute concentrations of colloidal ferrite (Fe_3O_4) MNPs ($\phi =$ 0.0005–0.005 v/v magnetic content) dispersed in water were prepared from commercial ferrofluid, EMG705 (FerroTec). The magnetic properties of EMG705 were measured by an alternating gradient magnetometer, MicroMag model 2900 (Princeton Instrument Co.) at 298 K in low-field (for initial susceptibility, χ_0) and high-field (for saturation magnetization, M_s) asymptote of magnetization curve (Hajiani and Larachi, 2012). Using these values, particle core diameter was estimated following a method proposed by Chantrell et al. (1978). Table 1 summarizes the magnetic properties of EMG-705 ferrofluid. The original ferrofluid supplied

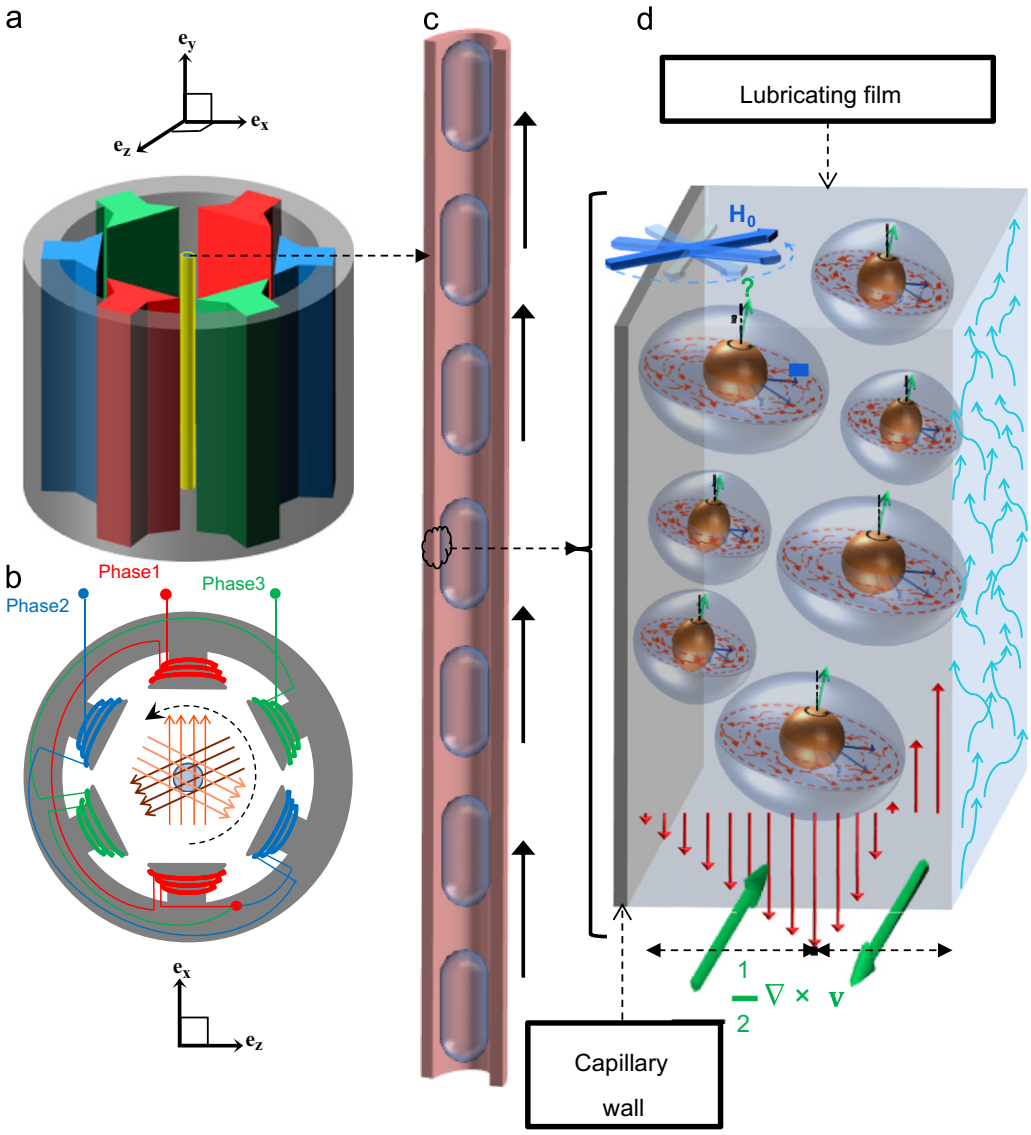

Fig. 1. Taylor bubbles in a tube exposed to magnetic field: (a) Experimental set-up including two-pole three-phase magnet and glass-made tube at the center; (b) upfront view of magnet with the tube set vertically and coaxially with magnet bore, and uniform *horizontal* magnetic field imposed across the tube hosting a flow of MNP-laden suspension; (c) rising Taylor bubbles in the tube; (d) expanded area of lubricating film where MNP spin plane is perpendicular to the tube wall.

from the company was diluted in deionized water to reach our prescribed concentrations.

2.3. Tube and magnetic field relative alignment

Theoretically, spinning rdMNPs dragged by a dynamic magnetic field (i.e., RMF and OMF) exchange angular momentum with liquid when particles spin *asynchronously* with respect to fluid vorticity ($1/2\nabla \times \mathbf{V}$) (Rosensweig, 1997). The fluid vorticity in the lubricating film of bubbles in Taylor flow regime is azimuthal while gas–liquid mass transfer occurs radially. Therefore, the tube was positioned coaxially with respect to the tubular magnet in transverse RMF (TRMF) to set the particle spin plane crosswise to the flow direction which is expected in turn to promote lateral mixing in the lubricating liquid film (Fig. 1c). Regarding the work of Shliomis and Morozov (1994), another conceivable configuration to enhance mass transfer in tube is when magnetically excited rdMNPs outpace fluid vorticity while they spin in parallel with it. They exemplified an OMF applied in parallel with a tube as a case and grounded the theoretical framework of MNPs dynamic behavior in such a system. Hence, the tube was also adjusted vertically and collinear with the magnetic field direction in the horizontal magnet (Fig. 4a). In contrast, SMF in the same tube-magnet configuration is postulated to pin all rdMNPs in the tube, making them resist against fluid vorticity (Fig. 5a). This configuration was used to explore the effect of MNP hindrance on gas–liquid mass transfer in the lubricating film.

2.4. Experimental setup

Taylor flow gas–liquid mass transfer experiments were carried out by means of oxygen absorption into MNP-water suspensions in two distinct tubes with circular cross-sections. The 4 mm I.D.-tube ($L=7$ cm) was positioned coaxially at the center of the magnet bore whereas the other with 2 mm I.D. ($L=4.5$ cm) was located transverse at the middle height of the magnet bore. The tube length was limited by the size of the magnet bore in both cases. A schematic diagram of the experimental set-up is shown in Fig. 2. Oxygen flow supplied from a gas cylinder was regulated through mass flow controller (Omega FMA14P). The designated flow of oxygen was directly fed into a T-shape plastic contactor inside the magnetic field where gas bubbles and liquid slugs form.

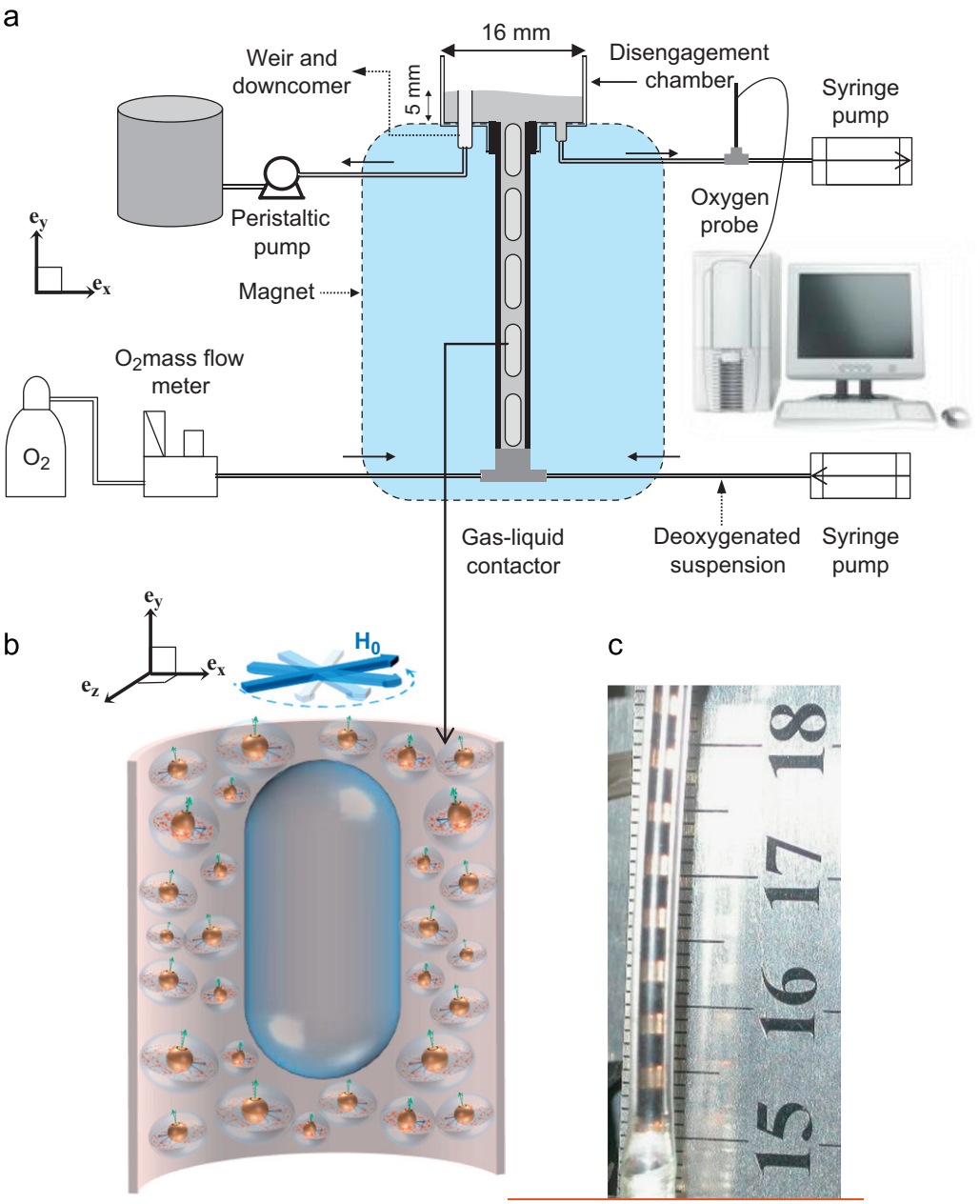

Fig. 2. (a) Experimental set-up for gas–liquid mass transfer study in tube; (b) single Taylor bubble surrounded by spinning MNPs in a TRMF; (c) Taylor flow of diluted ferrofluid observed in 2 mm I.D. tube, $U_g = 1.6$ cm/s and $U_L = 1.4$ cm/s.

Each batch of colloidal liquid phase was stripped out with pure nitrogen for at least three hours prior to each experiment to reach negligible initial oxygen concentration (i.e., less than 1 ppm). The magnetic properties of the suspension were verified to be unaltered by this pretreatment. A syringe pump with a range of 0–77.4 mL/min (Orion SAGE, Model 365) was used to deliver metered amounts of flow to the tube. The accurate liquid flow rate under each run was measured by weighting method. For each tube diameter, the gas and liquid flow were selected such that the flow regime in the tube turned into a sustainable Taylor flow regime (Fig. 2c) with partially oxygen-saturated lubricating films (Vandu et al., 2005). After passing the main tube, the multiphase mixture was directed immediately to a disengagement chamber connected to the tube end for phase separation. This phase separator was equipped with an outlet weir and downcomer tube which was itself connected to a peristaltic pump (Cole Palmer MasterFlex, Console Drive, Model 7521-50) for keeping the volume of the liquid constant at 1 mL during the course of experiment, corresponding to a liquid height of 5 mm as shown in Fig. 2a. Interferences between the magnetic field and the oxygen probe obligated installing this latter outside the disengagement chamber as shown in Fig. 2a. Therefore, a programmable inverted syringe pump was taking a sample from the bottom of disengagement cell once a minute and the dissolved oxygen content therein was analyzed by the oxygen probe (FOXY-R Stainless-steel, Fiber Optic Probe from Ocean Optics) on its passage. The oxygen content of the inlet suspension was measured prior to each run with a similar analysis without passing through the disengagement cell. All experiments were conducted under ambient conditions (101 kPa, 23–25 °C). Fig. 2b illustrates schematically the spinning MNPs around a single bubble when the system is subjected to the TRMF.

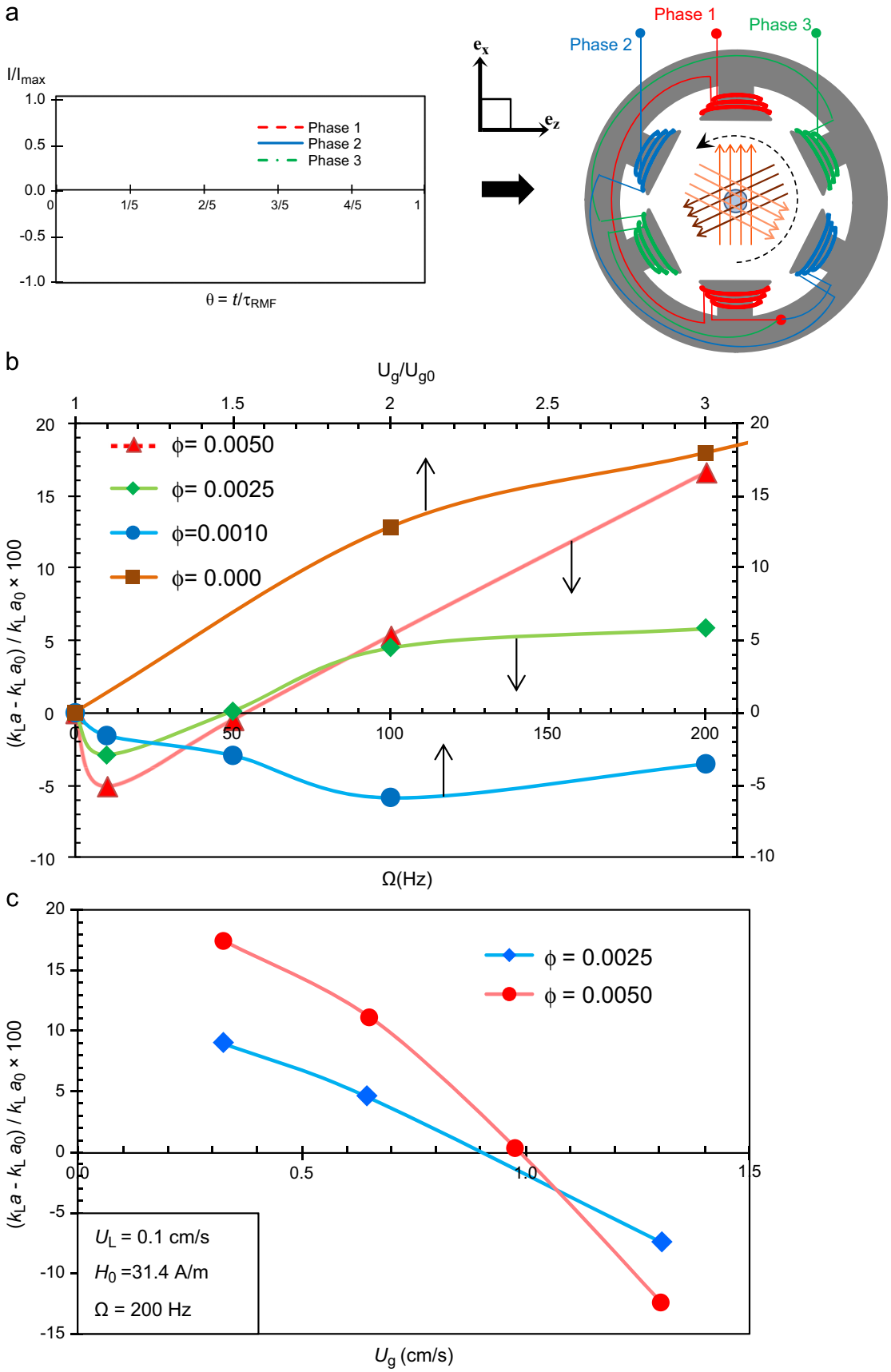

Fig. 3. (a) Glass tube located coaxially in the bore of a two-pole three-phase magnet (top view). Magnet generates a uniform rotating magnetic field (RMF) when energized by a three-phase power supply; (b) k_La enhancement factor as a function of TRMF frequency: For experiments under magnetic field (◆, ▲, ●), enhancement was due to TRMF and k_La_0 is mass transfer coefficient in absence of magnetic field for each particle concentration, U_L=0.1 cm/s, U_g=0.3 cm/s and H_0=31.4 kA/m. For k_La versus gas flow rate without magnetic field (■), enhancement originated from gas flow augmentation and k_La_0 corresponds to U_g=0.3 cm/s. Other parameters are the same (i.e., ϕ=0 and U_L=0.1 cm/s); (c) k_La enhancement factor under TRMF as a function of U_g for two MNP concentrations while U_L, H_0 and Ω were kept constant.

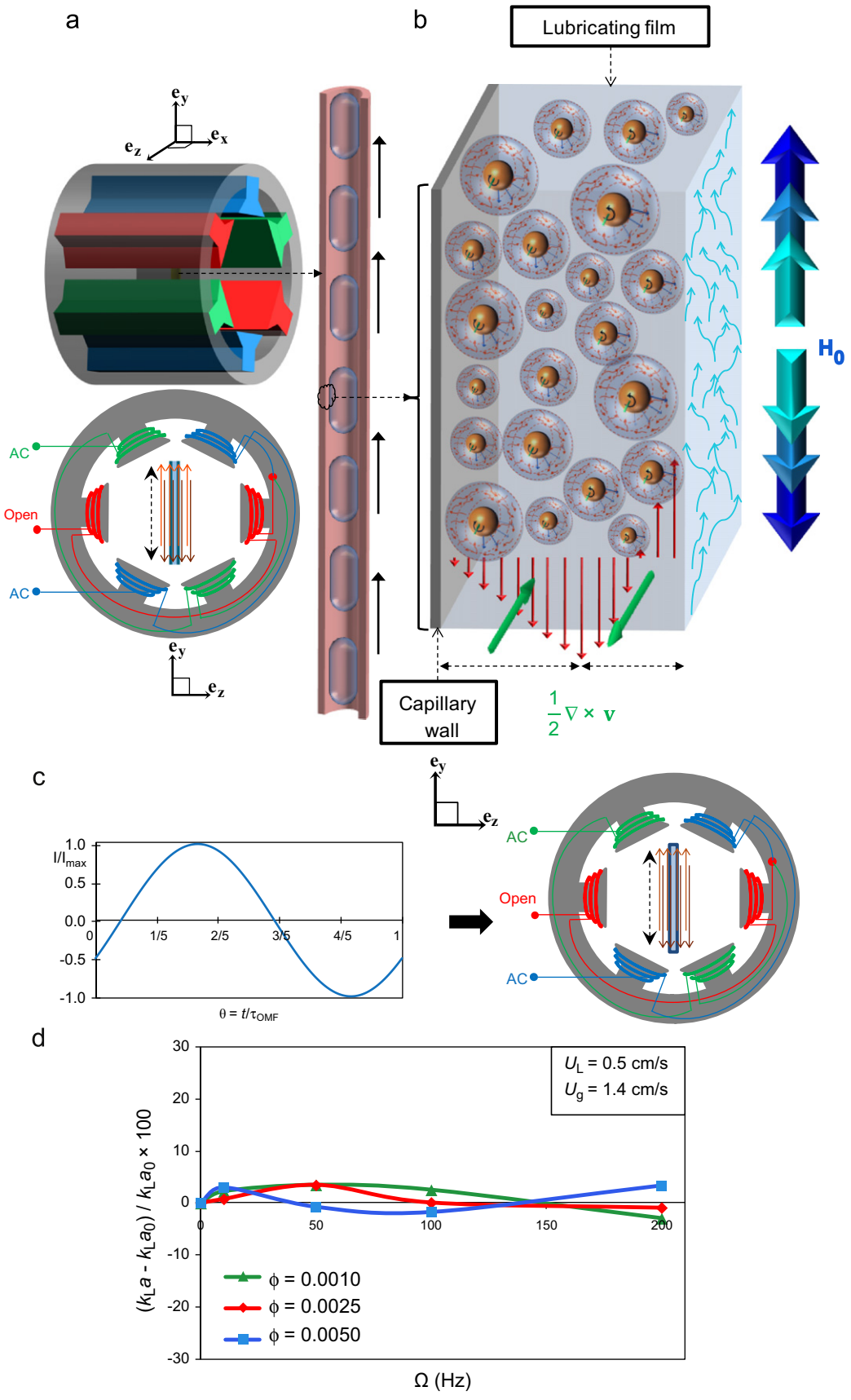

Fig. 4. (a) Side view of the magnet with a capillary tube which was set vertically and transverse with magnet bore, a uniform *vertical* magnetic field imposed along capillary tube; (b) rising Taylor bubbles surrounded with azimuthally spinning MNPs are shown. Fluid vorticity and consequently, particle spin vector inverted over film thickness; (c) the magnet generates a uniform oscillating magnetic field (OMF) when energized by an AC power supply; (d) k_La enhancement factor versus field frequency for three particle concentrations exposed to H_{0rms}=31.4 kA/m. k_La_0 is mass transfer coefficient for each particle concentration without magnetic field effect.

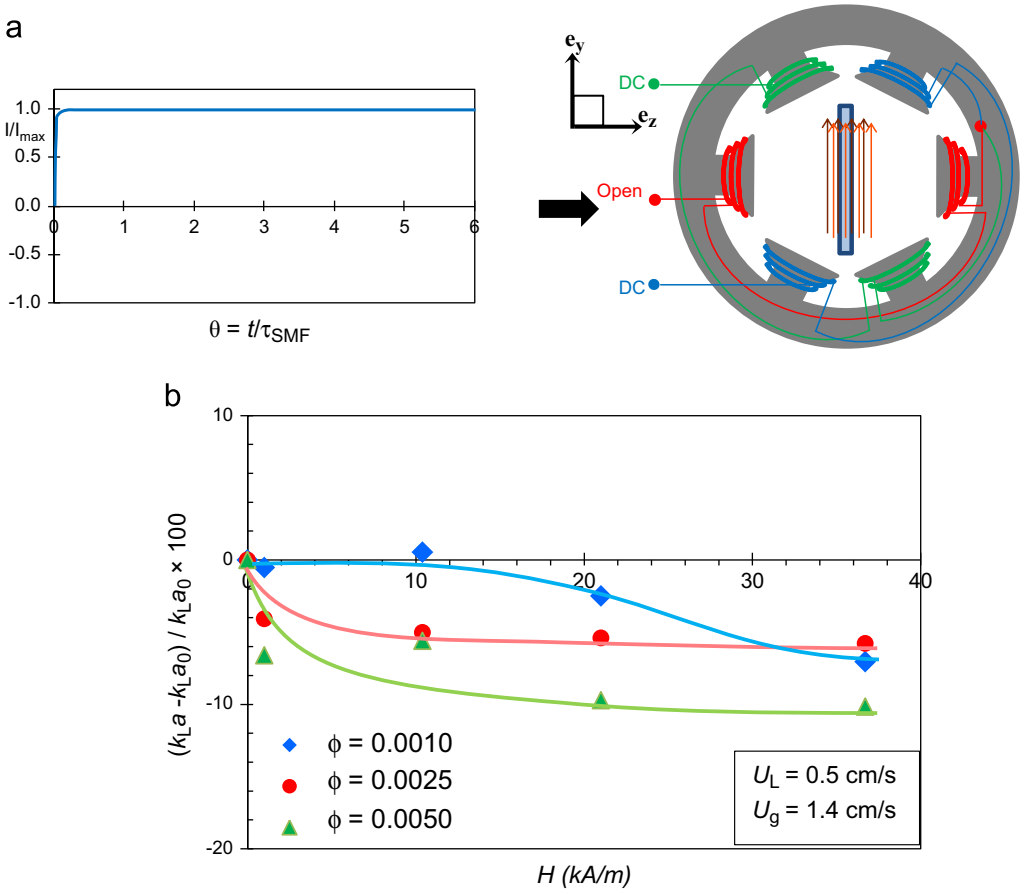

Fig. 5. (a) Capillary tube was located vertically in horizontal magnet (side view). The magnet generates a uniform stationary magnetic field (SMF) when energized by a DC power supply; (b) k_La enhancement factor versus field intensity for three particle concentrations. k_La_0 is suspension mass transfer coefficient for each particle concentration without magnetic field effect.

Table 1
Magnetic properties of EMG 705 from magnetometry measurement.

Saturation magnetization, M_s (kA/m)	18.7
Initial susceptibility, χ_0	2.9
MNP volume fraction, ϕ (v/v)	0.042
Estimated median magnetic core diameter, d_p (nm)	16.0

3. Results and discussion

Liquid side volumetric mass transfer (k_La) measurements were performed under three types of magnetic fields, i.e., transverse rotating magnetic field (TRMF), axial oscillating magnetic field (AOMF) and axial static magnetic field (ASMF). As explained above, the tube configuration was adapted with the desired spin direction of MNPs for each magnetic field type. Also, it is worth mentioning that the continuum hypothesis used to interpret our findings may not hold rigorously regarding MNPs actual diameter (~16 nm) or MNPs hydrodynamic diameter (~100 nm) since the Knudsen number with respect to the water molecules mean free path is less than 0.1 (Barber and Emerson, 2002).

3.1. Mass transfer enhancement in rotating magnetic field

Fig. 3a shows the configuration in which k_La measurements were made for dilute ferrofluids flowing through a vertical coaxial tube at the magnet bore center under TRMF. k_La enhancement factors versus magnetic field frequency (Ω_{RMF}) for several particle concentrations are shown in Fig. 3b. The figure demonstrates that for low field frequencies ($\Omega_{RMF} < 50$), the magnetic field tendency to spin MNPs is slower than the hydrodynamic propensity, due to fluid vorticity, to gyrate the MNPs. Consequently, the magnetic torque exerted on MNP slows down the fluid vorticity and partially retards the hydrodynamic mixing mechanism in the lubricating film. At higher frequencies, the faster particles spin intensifies liquid phase mixing and improves the mass transfer rate through a nanoconvective effect (Hajiani and Larachi, 2012). Moreover, the MNP concentration exacerbates both above-mentioned mechanisms (see Fig. 3b, $\phi = 0.0025, 0.0050$). As such, a more concentrated suspension leads to stronger mass transfer retardation in low frequencies and higher k_La enhancement in the high frequency region.

Complementarily, k_La enhancement under magnetic field effect was compared to k_La increase results merely from gas flow rate augmentation for $\phi = 0$ and $H_0 = 0$ kA/m (see Fig. 3b) while keeping the other operational conditions the same. The results indicate that the maximum mass transfer improvement achieved with the nanomixing mechanism (i.e., 16.5%) is attainable as well without any magnetic effect with three fold higher gas flow rate at the same liquid flow. Note that at the highest volume fraction $\phi = 0.0050$, an increase neither in gas flow rate nor in frequency were able to stimulate k_La under rotating magnetic field conditions ($H_0 = 31.4$ kA/m, Fig. 3b).

Fig. 3c gives another evidence of how the spinning magnetic nanoparticles interact with fluid vorticity to control mixing in the lubricating film. On the left side of the graph ($U_g < 1$ cm/s), the MNP spin dominates fluid vorticity which gives rise to an enhancement of k_La. By increasing the gas flow rate, the shear

rate on the gas–liquid interface results in higher fluid vorticity that surpasses MNP spin and thus undermines the transverse nanoconvective effect. On the right side of Fig. 3c, fluid vorticity outweighs nanoparticle spin and results in downgrading the gas–liquid mass transfer compared to its magnetic field free counterpart. Both spin-dominant (lower U_g) and vorticity-dominant (higher U_g) effects are likely magnified at higher MNP concentration (Fig. 3c).

The aggregate of observations discussed under Fig. 3 implies that there is an intrinsic disadvantage of having the MNPs spin in a plane perpendicular to the fluid vorticity in the liquid film. From both stagnant film theory (Whitman, 1923) or penetration theory (Danckwerts and Kennedy, 1954; Higbie, 1935) it may be concluded that apart from molecular diffusion, fluid vorticity is the only mixing mechanism of the liquid bulk in gas–liquid contactor. Hence, the fact that TRMF opposes fluid vorticity is in contradiction with the ultimate goal of k_La enhancement. This notion is conceivable from Fig. 3c and is reinforced from Fig. 3b results as at low frequencies, k_La decreases in presence of particle spin. Increasing the field frequency will strengthen the restrictive effect of spinning MNPs on vorticity. However, strong nano-stirring in higher frequencies compensates the lack of vorticity-based mixing and slightly modifies k_La.

3.2. Mass transfer under an oscillating magnetic field

A substitution approach would be to force MNPs to spin in parallel with fluid vorticity. Such particles spin, ω, when becoming fast enough, i.e., $\omega > 1/2|\nabla \times \mathbf{V}|$, may intensify mixing without restraining fluid vorticity. In this case, nano-convective effect does not necessarily inhibit the vorticity in order to play a role in liquid film agitation, as it does under TRMF. According to the azimuthal direction of fluid vorticity in liquid film within the tube, the particle spin vector should be azimuthal as well. Furthermore, the vorticity vector changes sign over film thickness where the liquid film velocity reaches maximum as illustrated in Fig. 4b. Therefore, the direction of particle spin vector must be reversed locally over that hypothetical hydrodynamic boundary which is set by the direction of fluid vorticity. In this view, the advantages obtained by applying an AOMF would be twofold. Particle spin vector (ω) is favorably azimuthal under AOMF in cylindrical geometry (Bacri et al., 1995; Shliomis and Morozov, 1994). Moreover, since the sign of ω is at discretion of the fluid vorticity (Shliomis and Morozov, 1994), the particle spin is entirely synchronous with fluid vorticity over entire liquid film.

To establish AOMF conditions, we used a capillary ($d=2$ mm, $L=4.5$ cm) which was set vertically at the center of horizontal magnet bore (Fig. 4a). Four coils, which were connected in series, were energized with an AC electrical current from a variable frequency drive (ABB, ACS150, 2.2 kW) to generate AOMF (Fig. 4c). Fig. 4d shows k_La enhancement factor of three MNP concentrations versus field frequencies with $H_{0\mathrm{rms}}$ of 31.4 kA/m. As seen, insignificant mass transfer enhancement under AOMF did not comply with our expectation in the framework explained in Fig. 4b. According to the small particle size ($d_p=16.0$ nm) and extremely low field frequency ($\Omega < 300$ Hz), the underlying cause of this result would be the intrinsic inability of low frequency OMF to bring rdMNP into consistent full rotation. Brownian agitation interference or the effect of strong hydrodynamic torque at the very brief moment when OMF pass through zero intensity during each wave cycle may have inhibited the synchronized rotation of MNPs under OMF in our experiments. Larger MNPs (Gazeau et al., 1997) or much higher frequencies ($\Omega > 10^5$ Hz) (Bacri et al., 1995; Schumacher et al., 2003; Zeuner et al., 1998) are perceived to be required. Such a high frequency does not match with the design of our present magnet setup. However, having larger MNPs would be regarded as a rational solution to this challenge.

3.3. Mass transfer under a static magnetic field

Finally, we investigated the effect of magnetically locked MNPs (magnetoviscosity) on k_La in the Taylor flow regime. The tube in the same configuration as in Fig. 4a was subjected to a uniform static magnetic field (SMF) which was generated by four coils energized by a DC power supply (Fig. 5a). As k_La declines versus H_0 and MNP concentration in Fig. 5b, the results indicate that magnetically pinned MNPs incapacitate gas–liquid mass transfer systematically. In fact, pinned MNPs prevent liquid layers from free sliding on top of each other under viscid flow. This phenomenon impairs mixing or surface renewal in liquid film around the rising bubble to a certain extent. Besides, it may lessen liquid recirculation in the slug due to inflated viscosity. Therefore, k_La reduction observed in Fig. 5b may be attributed to the aggregate effects of magnetically locked MNPs around the bubbles and in the liquid slugs.

4. Conclusion

By studying k_La in a Taylor flow system comprising dilute aqueous colloidal suspension of MNPs and oxygen bubbles under moderate strength TRMF, AOMF and ASMF, we investigated the effects resulting from nanoparticle magnetic torque exchange with liquid phase on the gas–liquid mass transfer. The nature of these effects in a two-phase system was found to be similar to that in single-phase systems. Our results demonstrated k_La enhancement due to nanoconvective stirring induced by excited MNPs under TRMF. Moreover, it provided clear evidence of the interaction between magnetic torque and fluid vorticity as contributing to two distinctive competing mixing mechanisms while indicating the conditions in which either of them prevails.

By contrast, no significant mass transfer enhancement could be seen under low frequency AOMF, probably due to the small particle size or extremely low field frequency. Further studies are required to identify the optimal particle size or field frequency that sustains full synchronized spin of MNPs driven by AOMF. Finally, reductions in k_La were also observed while the tube was subjected to ASMF. This observation confirms earlier reports on inhibitive role of magnetically pinned MNPs on mass transfer phenomenon in diluted colloidal systems (Hajiani and Larachi, 2012). In sum, our experimental results point out further evidences that MNPs, excited by appropriate magnetic field, manipulate liquid transport properties in a variety of flowing systems. However, nanomixing application for liquid mass transfer enhancement would be limited to those systems in which hydrodynamic torque, originating from fluid vorticity, has the same magnitude relative to magnetic torque on MNP which is imposed by time varying magnetic fields.

Nomenclature

d	Tube diameter (mm)
d_p	Volume median particle diameter (m)
H_0	External (imposed) magnetic field intensity (A/m)
k_La	Liquid side volumetric mass transfer (1/s)
L	Tube length (cm)
rdMNP	Rigid dipole magnetic nanoparticle
U_g	Gas superficial velocity (cm/s)
U_L	Liquid superficial velocity (cm/s)

Greek

ω	MNP spin velocity vector per unit volume (rad/s)
Ω	Magnetic field frequency (Hz)
τ_{RMF}	Rotating magnetic field time constant $=1/\Omega_{RMF}$ (s)
τ_{OMF}	Oscillating magnetic field time constant $=1/\Omega_{OMF}$ (s)
τ_{SMF}	Static magnetic field time constant $=1$ s
ϕ	MNP core volume fraction
$1/2\nabla\times\mathbf{V}$	Fluid vorticity vector $=s^{-1}$

Acronyms

MNP	Magnetic nanoparticle
OMF	Oscillating magnetic field
RMF	Rotating magnetic field
SMF	Static (DC) magnetic field

Acknowledgements

Support from the Natural Sciences and Engineering Research Council of Canada and the Canada Research Chair "Green processes for cleaner and sustainable energy" is gratefully acknowledged. The authors also thank A. Faridkhou for helpful editing assistance and O. Gravel for assistance in preparing the set-up.

References

Bacri, J.C., Perzynski, R., Shliomis, M.I., Burde, G.I., 1995. Negative-viscosity effect in a magnetic fluid. Phys. Rev. Lett. 75, 2128–2131.

Barber, R.W., Emerson, D.R., 2002. The influence of Knudsen number on the hydrodynamic development length within parallel plate micro-channels. In: Rahman, M., Verhoeven, R., Brebbia, C.A. (Eds.), Advances in Fluid Mechanics IV. WIT Press, Southampton, UK, pp. 207–216.

Chantrell, R.W., Popplewell, J., Charles, S.W., 1978. Measurements of particle-size distribution parameters in ferrofluids. IEEE Trans. Magn. 14, 975–977.

Danckwerts, P.V., Kennedy, A.M., 1954. Kinetics of liquid-film process in gas absorption. part 1: Models of the absorption process. Trans. Am. Inst. Chem. Eng. 32, S101–S104.

De Mas, N., Gunther, A., Schmidt, M.A., Jensen, K.F., 2009. Increasing productivity of microreactors for fast gas––liquid reactions: the case of direct fluorination of toluene. Ind. Eng. Chem. Res. 48, 1428–1434.

Du, X.Y., He, J., Zhu, J., Sun, L.J., An, S.S., 2012. Ag-deposited silica-coated Fe_3O_4 magnetic nanoparticles catalyzed reduction of *p*-nitrophenol. Appl. Surf. Sci. 258, 2717–2723.

Fu, Y.S., Chen, H.Q., Sun, X.Q., Wang, X., 2012. Combination of cobalt ferrite and graphene: high-performance and recyclable visible-light photocatalysis. Appl. Catal., B 111, 280–287.

Gazeau, F., Baravian, C., Bacri, J.C., Perzynski, R., Shliomis, M.I., 1997. Energy conversion in ferrofluids: magnetic nanoparticles as motors or generators. Phys. Rev. E 56, 614–618.

Gong, X.Q., Miller, P.W., Gee, A.D., Long, N.J., De Mello, A.J., Vilar, R., 2012. Gas–liquid segmented flow microfluidics for screening Pd-catalyzed carbonylation reactions. Chem. Eur. J. 18, 2768–2772.

Gunther, A., Khan, S.A., Thalmann, M., Trachsel, F., Jensen, K.F., 2004. Transport and reaction in microscale segmented gas–liquid flow. Lab. Chip. 4, 278–286.

Hajiani, P., Larachi, P., 2012. Reducing Taylor dispersion in capillarylaminarflows using magnetically excited nanoparticles: nanomixing mechanism for micro/nanoscale applications. Chem. Eng. J. 203, 492–498.

Hessel, V., Angeli, P., Gavriilidis, A., Lowe, H., 2005. Gas–liquid and gas–liquid–solid microstructured reactors: contacting principles and applications. Ind. Eng. Chem. Res. 44, 9750–9769.

Higbie, R., 1935. The rate of absorption of a pure gas into a still liquid during short periods of exposure. Trans. Am. Inst. Chem. Eng. 31, 365–389.

Hudson, R., Li, C.J., Moores, A., 2012. Magnetic copper–iron nanoparticles as simple heterogeneous catalysts for the azide–alkyne click reaction in water. Green Chem. 14, 622–624.

Kashid, M.N., Renken, A., Kiwi-Minsker, L., 2011. Gas–liquid and liquid–liquid mass transfer in microstructured reactors. Chem. Eng. Sci. 66, 3876–3897.

Kong, A.G., Wang, P., Zhang, H.G., Yang, F., Huang, S.P., Shan, Y.K., 2012. One-pot fabrication of magnetically recoverable acid nanocatalyst, heteropolyacids/chitosan/Fe_3O_4, and its catalytic performance. Appl. Catal., A 417, 183–189.

Lang, P., Hill, M., Krossing, I., Woias, P., 2012. Multiphase minireactor system for direct fluorination of ethylene carbonate. Chem. Eng. J. 179, 330–337.

Liu, Y.H., Deng, J., Gao, J.W., Zhang, Z.H., 2012. Triflic acid-functionalized silica-coated magnetic nanoparticles as a magnetically separable catalyst for synthesis of gem-dihydroperoxides. Adv. Synth. Catal. 354, 441–447.

McTague, J.P., 1969. Magnetoviscosity of magnetic colloids. J. Chem. Phys. 51, 133–136.

Ng, J.F., Nie, Y., Chuah, G.K., Jaenicke, S., 2010. A wall-coated catalytic capillary microreactor for the direct formation of hydrogen peroxide. J. Catal. 269, 302–308.

Ngo, T.P.N., Zhang, W., Wang, W., Li, Z., 2012. Reversible clustering of magnetic nanobiocatalysts for high-performance biocatalysis and easy catalyst recycling. Chem. Commun. 48, 4585–4587.

Rosensweig, R.E., 1997. Ferrohydrodynamics, N.Y. Dover Publications, Mineola.

Rosensweig, R.E., Kaiser, R., Miskolcz, G., 1969. Viscosity of magnetic fluid in a magnetic field. J. Colloid Interface Sci. 29, 680.

Sato, M., Goto, M., 2004. Gas absorption in water with microchannel devices. Sep. Sci. Technol. 39, 3163–3167.

Schumacher, K.R., Sellien, I., Knoke, G.S., Cader, T., Finlayson, B.A., 2003. Experiment and simulation of laminar and turbulent ferrofluid pipe flow in an oscillating magnetic field. Phys. Rev. E 67, 11.

Shliomis, M.I., Morozov, K.I., 1994. Negative viscosity of ferrofluid under alternating magnetic-field. Phys. Fluids 6, 2855–2861.

TeGrotenhuis, W.E., Cameron, R.J., Viswanathan, V.V., Wegeng, R.S., 2000. Solvent Extraction and Gas Absorption Using Microchannel Contactors. Microreaction Technology: Industrial Prospects. 541-549.

Trachsel, F., Gunther, A., Khan, S., Jensen, K.F., 2005. Measurement of residence time distribution in microfluidic systems. Chem. Eng. Sci. 60, 5729–5737.

Vandu, C.O., Liu, H., Krishna, R., 2005. Mass transfer from Taylor bubbles rising in single capillaries. Chem. Eng. Sci. 60, 6430–6437.

Wang, X., Nie, Y.T., Lee, J.L.C., Jaenicke, S., 2007. Evaluation of multiphase microreactors for the direct formation of hydrogen peroxide. Appl. Catal., A 317, 258–265.

Whitman, W.G., 1923. A preliminary experimental confirmation of the two-film theory of gas absorption. Chem. Metall. Eng. 29, 146–148.

Xu, H.J., Wan, X., Shen, Y.Y., Xu, S., Feng, Y.S., 2012. Magnetic nano-Fe_3O_4-supported 1-benzyl-1,4-dihydronicotinamide (BNAH): synthesis and application in the catalytic reduction of alpha, beta-epoxy ketones. Org. Lett. 14, 1210–1213.

Yue, J., Chen, G.W., Yuan, Q., Luo, L.G., Gonthier, Y., 2007. Hydrodynamics and mass transfer characteristics in gas–liquid flow through a rectangular microchannel. Chem. Eng. Sci. 62, 2096–2108.

Zaloha, P., Kristal, J., Jiricny, V., Volkel, N., Xuereb, C., Aubin, J., 2012. Characteristics of liquid slugs in gas–liquid Taylor flow in microchannels. Chem. Eng. Sci. 68, 640–649.

Zeuner, A., Richter, R., Rehberg, I., 1998. Experiments on negative and positive magnetoviscosity in an alternating magnetic field. Phys. Rev. E 58, 6287–6293.

Zhang, F.W., Niu, J.R., Wang, H.B., Yang, H.L., Jin, J., Liu, N., Zhang, Y.B., Li, R., Ma, J.T., 2012a. Palladium was supported on superparamagnetic nanoparticles: a magnetically recoverable catalyst for Heck reaction. Mater. Res. Bull. 47, 504–507.

Zhang, Q., Su, H., Luo, J., Wei, Y.Y., 2012b. A magnetic nanoparticle supported dual acidic ionic liquid: a "quasi-homogeneous" catalyst for the one-pot synthesis of benzoxanthenes. Green Chem. 14, 201–208.

Zhu, C.J., Wei, Y.Y., 2012. Facile preparation and reactivity of magnetic nanoparticle- supported hypervalent iodine reagent: a convenient recyclable reagent for oxidation. Adv. Synth. Catal. 354, 313–320.